

**Figure 1:** a - Study area location and Campi Flegrei area. b – Study area detailed orthophoto (2004) (<https://sit2.regione.campania.it/content/ortofoto-campania-20042005>).

**Figure 2:** Coroglio cliff view from WSW. Red dashed line shows the area mapped in Fig. 3; yellow dotted line shows the area involved by reinforcement works; light blue circle shows the area with unstable tuff blocks; red arrow shows the detachment area of the failure occurred around 1990, located outside the area mapped in Fig.3. Black lines separate upper, median and lower parts of the cliff.

**Figure 3:** Geological vertical map of the Coroglio cliff (modified after Matano et al., 2016). Landslide types occurred during 2013-2015 interval (Caputo et al., 2018) are also showed. Geological units: LP, stiff to loose recent pyroclastic deposits and soils; LP-NYT, thin layer of LP deposits on NYT unit; NYT, Neapolitan Yellow Tuff; TTR, Trentaremi Tuff; dt, slope talus breccia and gravelly beach deposits.

**Figure 4:** Geostructural vertical map (modified by Matano et al., 2016). Black boxes show location of the monitored unstable tuff blocks. Set legend (dip/dip direction): F1a (>65°/30-50° and 220-235°), F1b (>65°/50-60° and 235-245°), F1c (>65°/55-65° and 245-255°), F2 (>65°/0-30° and 180-220°), F3 (>70°/60-110° and 255-280°), F4 (>70°/110-180° and 300-355°), F5 (20-65°/50-195°), F6 (< 20°/0-360°).

**Figure 5:** Unstable tuff blocks of the NYT unit selected for monitoring activity (red lines).

**Figure 6:** Data distribution of measurements of crackmeters (03F1, 04F1, 05F1, 05F2, 05F3, 16F1, 16F2, 19F1 and 19F2).

**Figure 7:** Correlation plot between 05F1 and 05F3 data.

**Figure 8:** Data distribution of measurements of tiltmeters (04I2-X, 04I2-Y, 19I3-X and 19I3-Y).

**Figure 9:** Data distribution of measurements of thermistors (19I3-T, 04I2-T and Temp-1).

**Figure 10:** Temperature time series showing daily, seasonal and annual variation patterns. Long-term trends, based on about five consecutive years of data, show annual cyclicity. Air temperature and near-rock-surface air temperature are fully synchronous; peaks in near-rock-surface air temperatures (19I3-T, 04I2-T and Temp-1) are sometimes higher than those of air temperature (Temp). Data are incomplete in some months.

**Figure 11:** Crack aperture variation time series showing daily, seasonal and annual deformation patterns. Long-term trends, based on about four consecutive years of data (December 2014 to October 2018), show from +0,1 to +1,2 mm cumulative deformation. Data are incomplete in some months.

**Figure 12:** Angle variation time series data showing daily, seasonal and annual deformation patterns. Long-term trends, based on about four consecutive years of data (December 2014 to October 2018), show from 0,1° to 0,4° cumulative angle variation. Horizontal and vertical angle variation show opposite evidences for each block. Data are incomplete in some months.

**Figure 13:** Annual time series plots of 05F2 crackmeter showing partly repetitive seasonal deformation patterns.

**Figure 14:** Average daily thermal trend, referred to 2014-2018, recorded by Denza weather station with 4<sup>th</sup> grade polynomial equation. Maximum temperature values are indicated with red line, minimum values with blue line and daily temperature range with green line.

**Figure 15:** Rain amount (10 minutes) and rain rate time series data showing daily, seasonal and annual variation patterns in the Denza station during 2014-2018.

**Figure 16:** Average cumulative monthly rainfall data histogram referred to 2014-2018. Diagram reports also average monthly values of rainfall, measured at Meteorological Observatory of University of Naples “Federico II” since 1872 (Mazzarella, 2006). Rainfall values are reported, respectively, in blue squared cells and red squared cells.

**Figure 17:** Wind and gust speed time series data showing daily, seasonal and annual variation patterns in the Denza station during 2014-2018.

**Figure 18:** Frequency distribution of wind and gust directions measured during 2014-2018.

**Figure 19:** Wind and gust normal pressure time series data showing daily, seasonal and annual variation patterns in the Denza station during 2014-2018.

**Figure 20:** Barometric pressure and humidity time series data showing seasonal and annual variation patterns in the Denza station during 2014-2018.

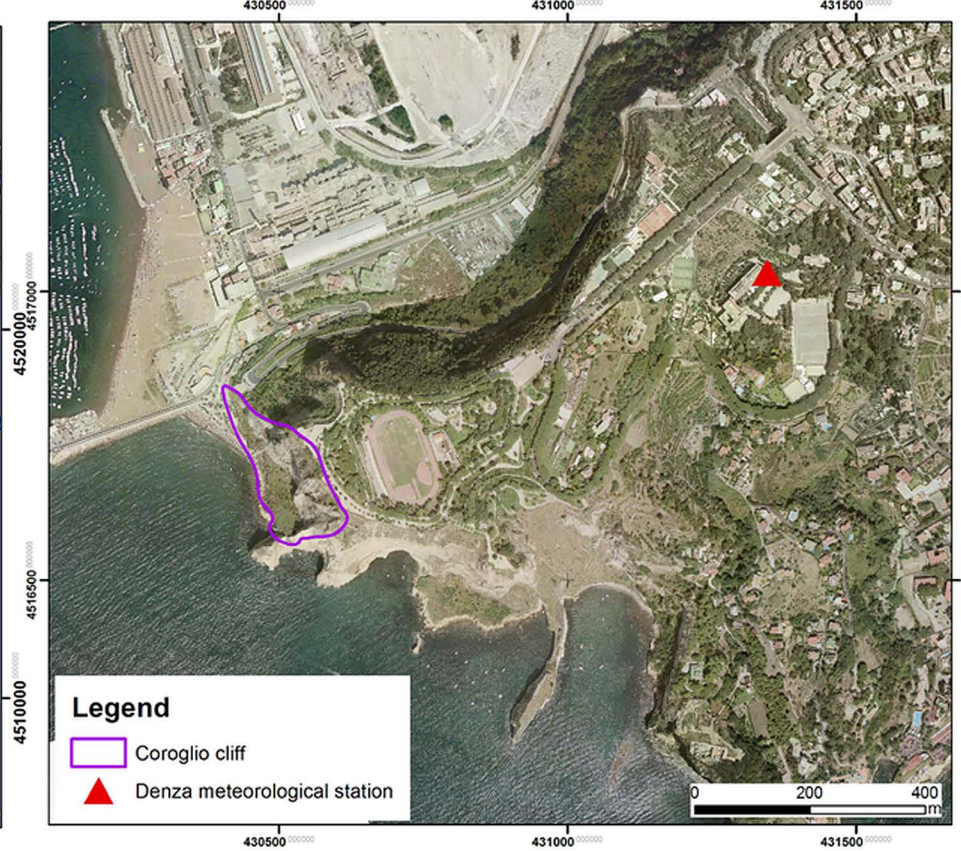
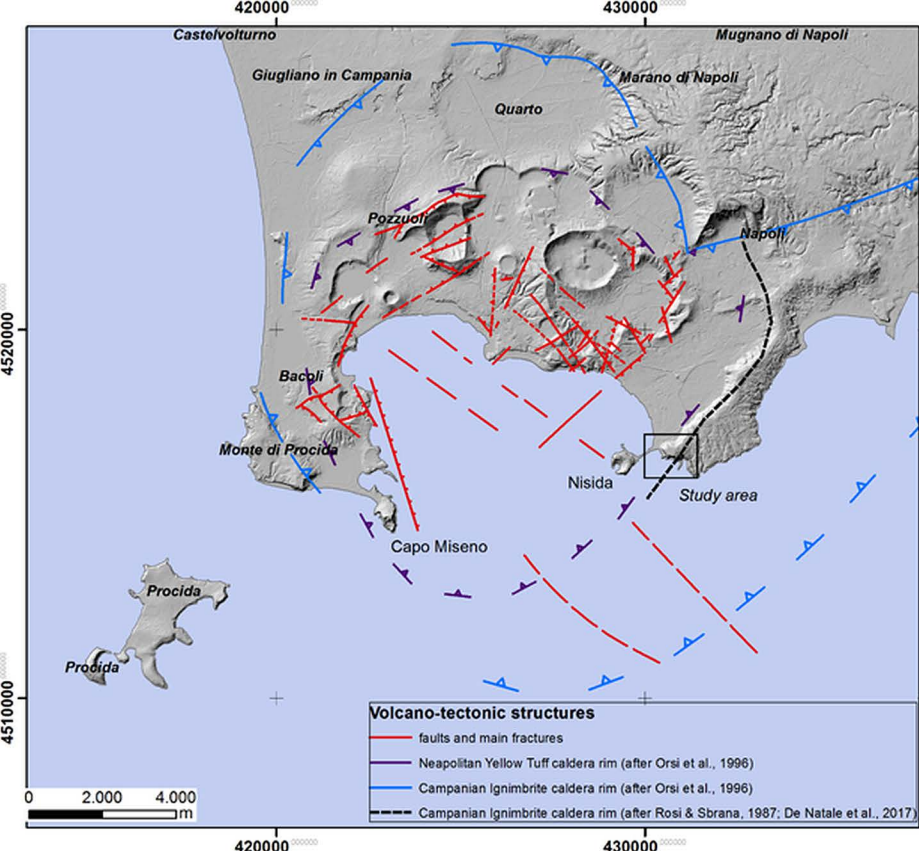
**Figure 21:** Comparison between crackmeter measurements, rain amount and temperature daily data time series.

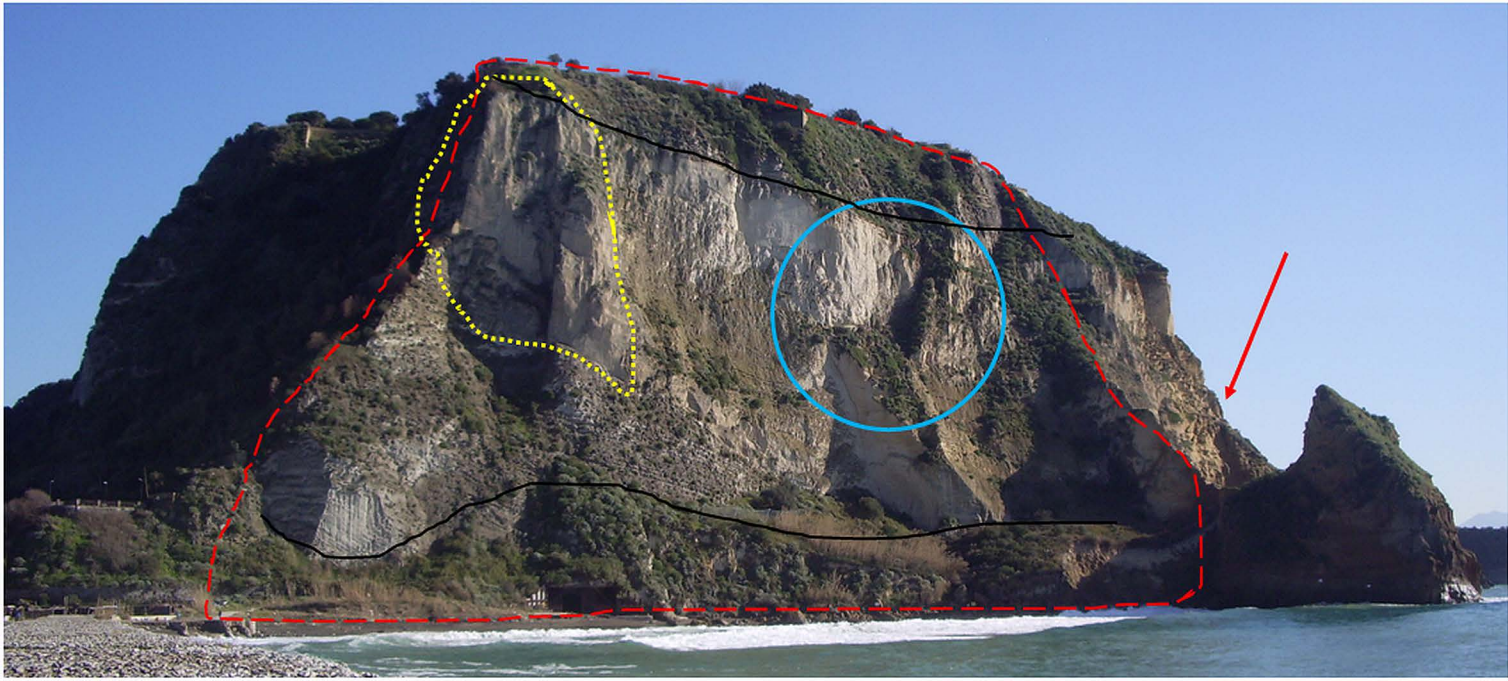
**Figure 22:** Comparison between crackmeter measurements and maximum rain rate daily data time series.

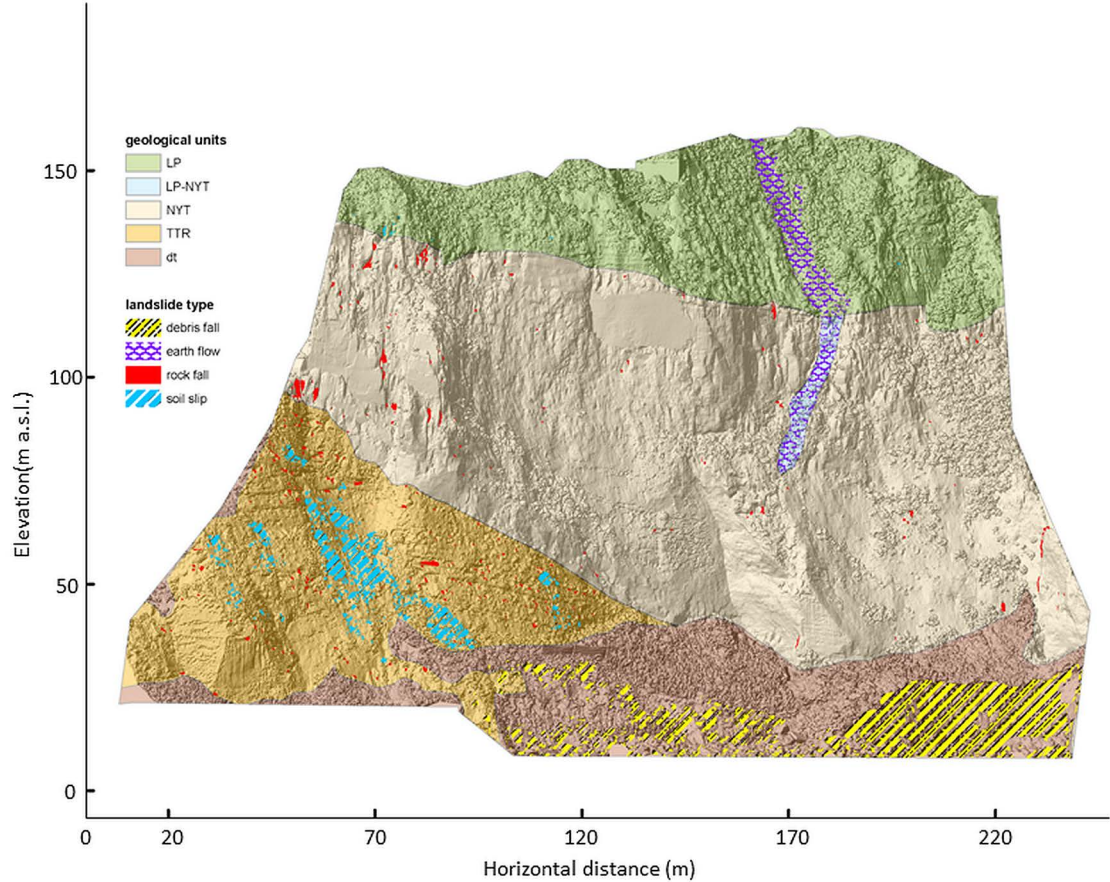
**Figure 23:** Comparison between crackmeter measurements and wind (wind speed, gust speed, wind normal pressure, gust normal pressure) daily data time series.

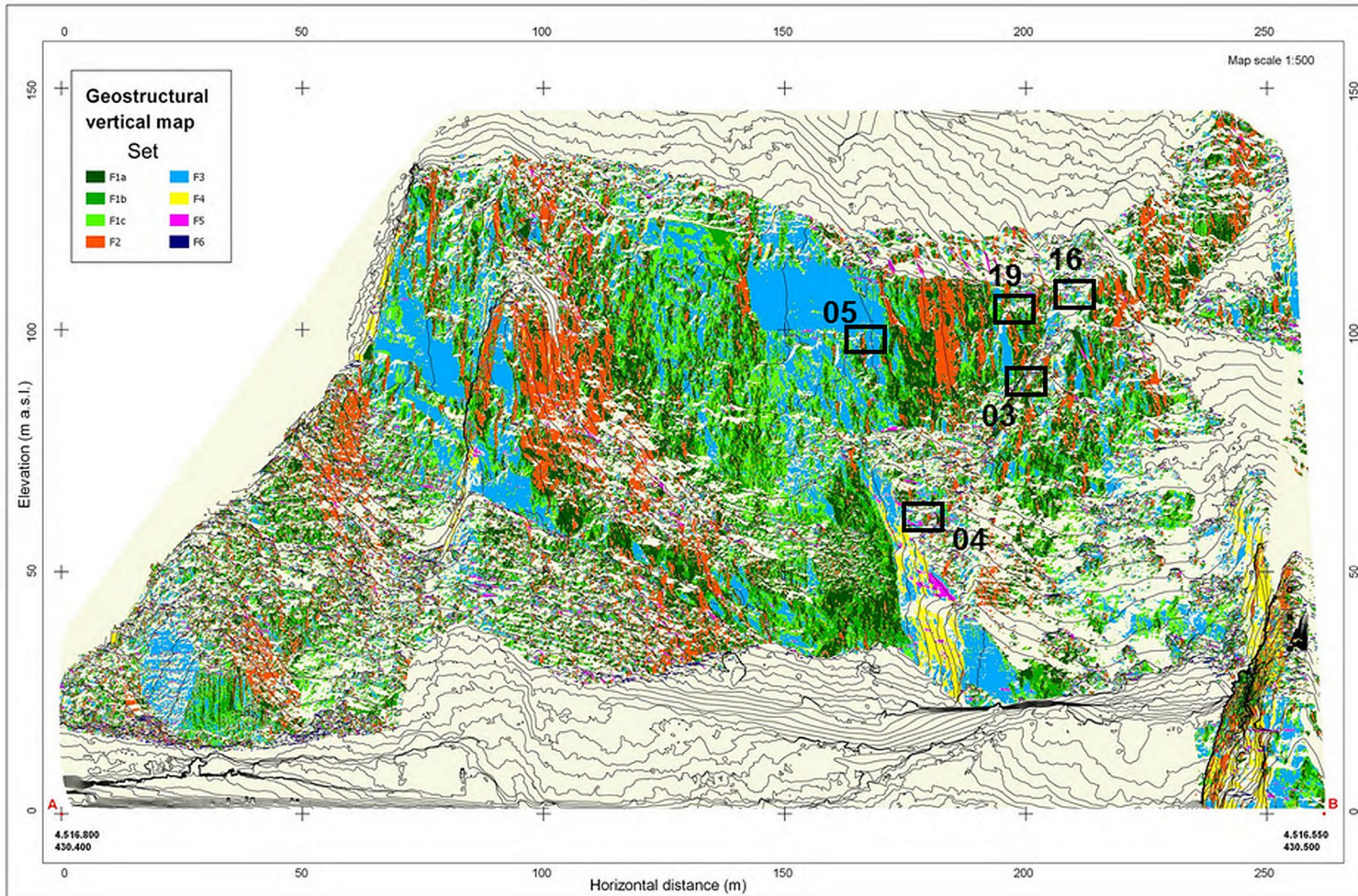
**Figure 24:** Comparison between crackmeter measurements, relative humidity and barometric pressure) daily data time series.

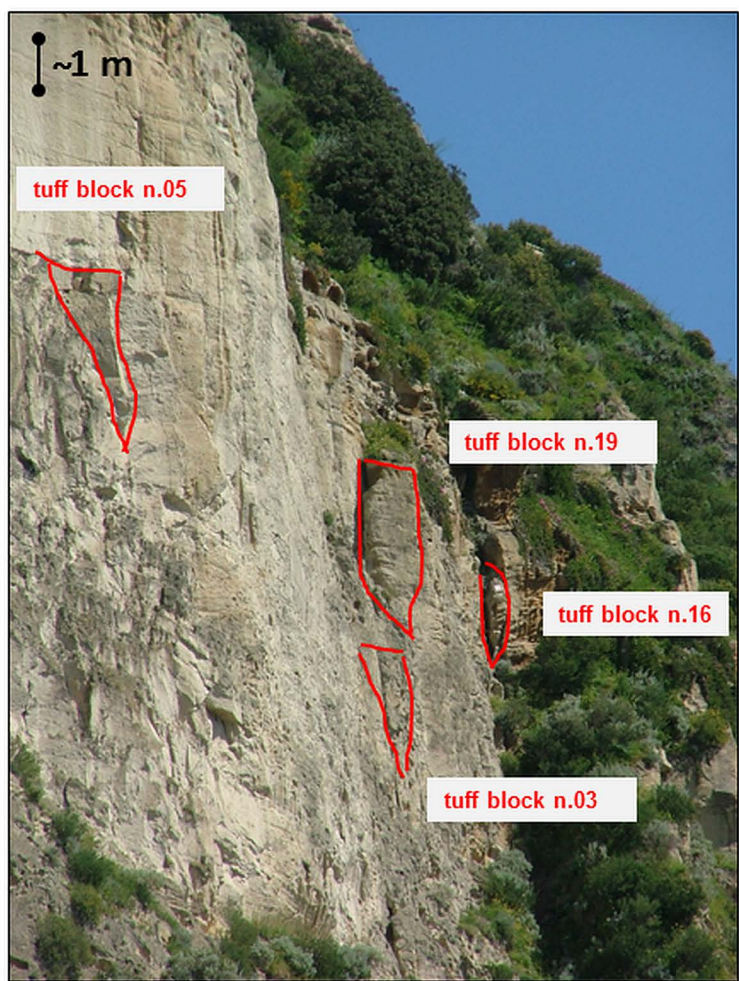
**Figure 25:** Progressive increase of tiltmeter F19I3-Y measurements values (see dashed arrows) from 2015 to 2018 referred to local temperature.

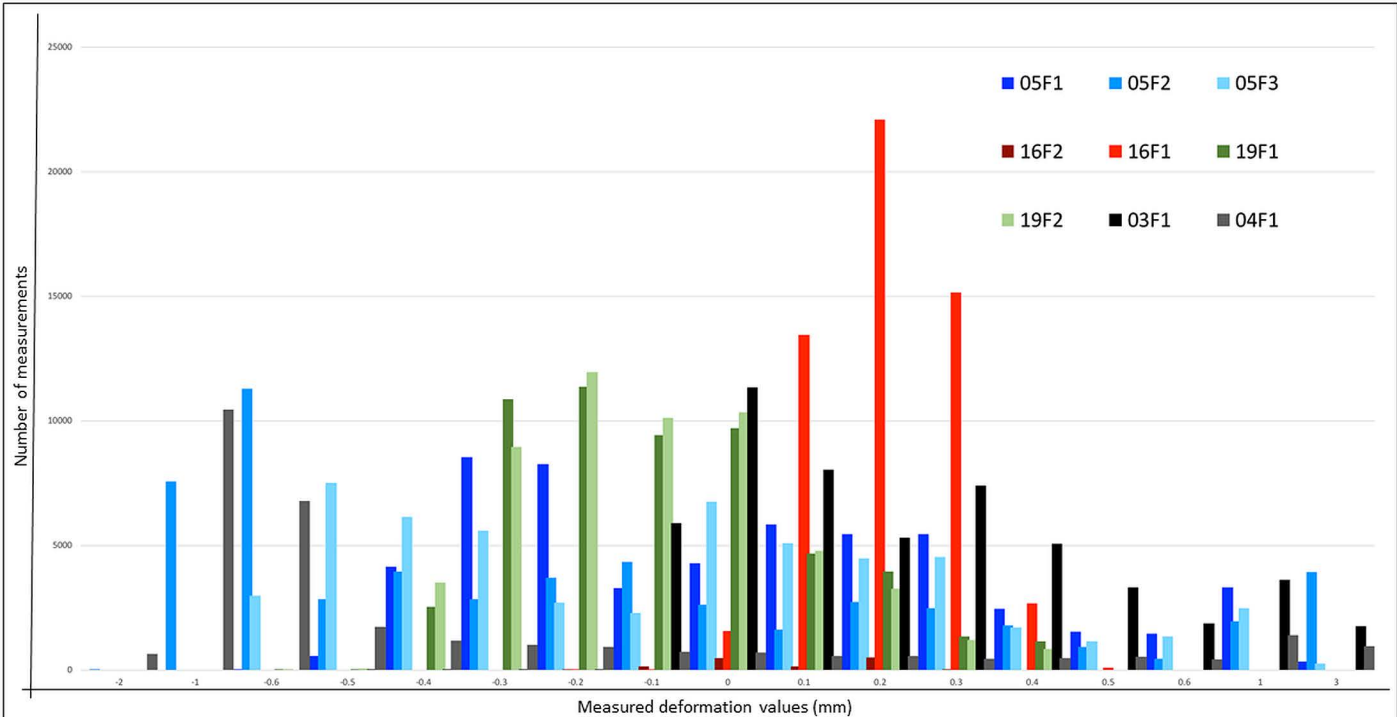


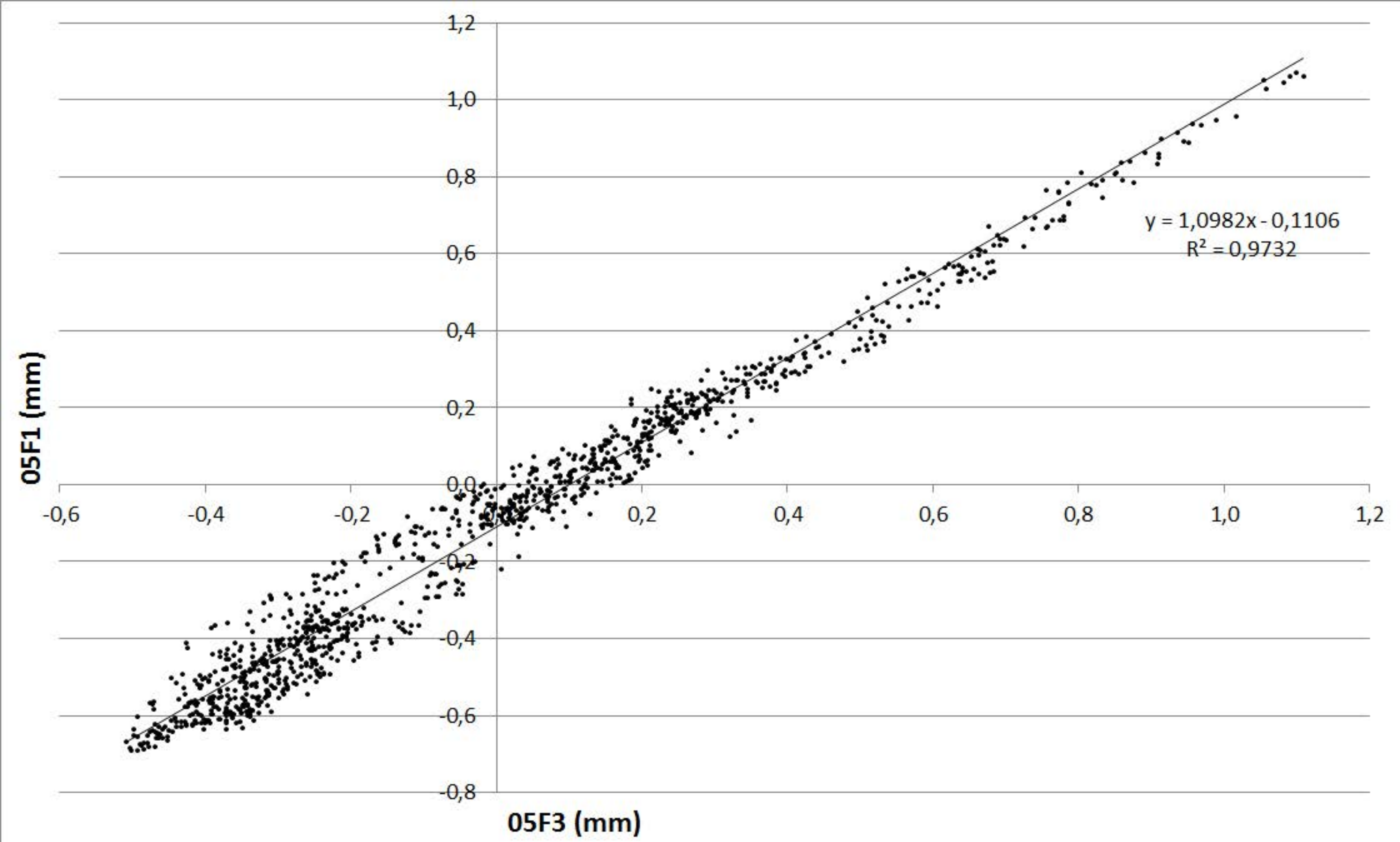


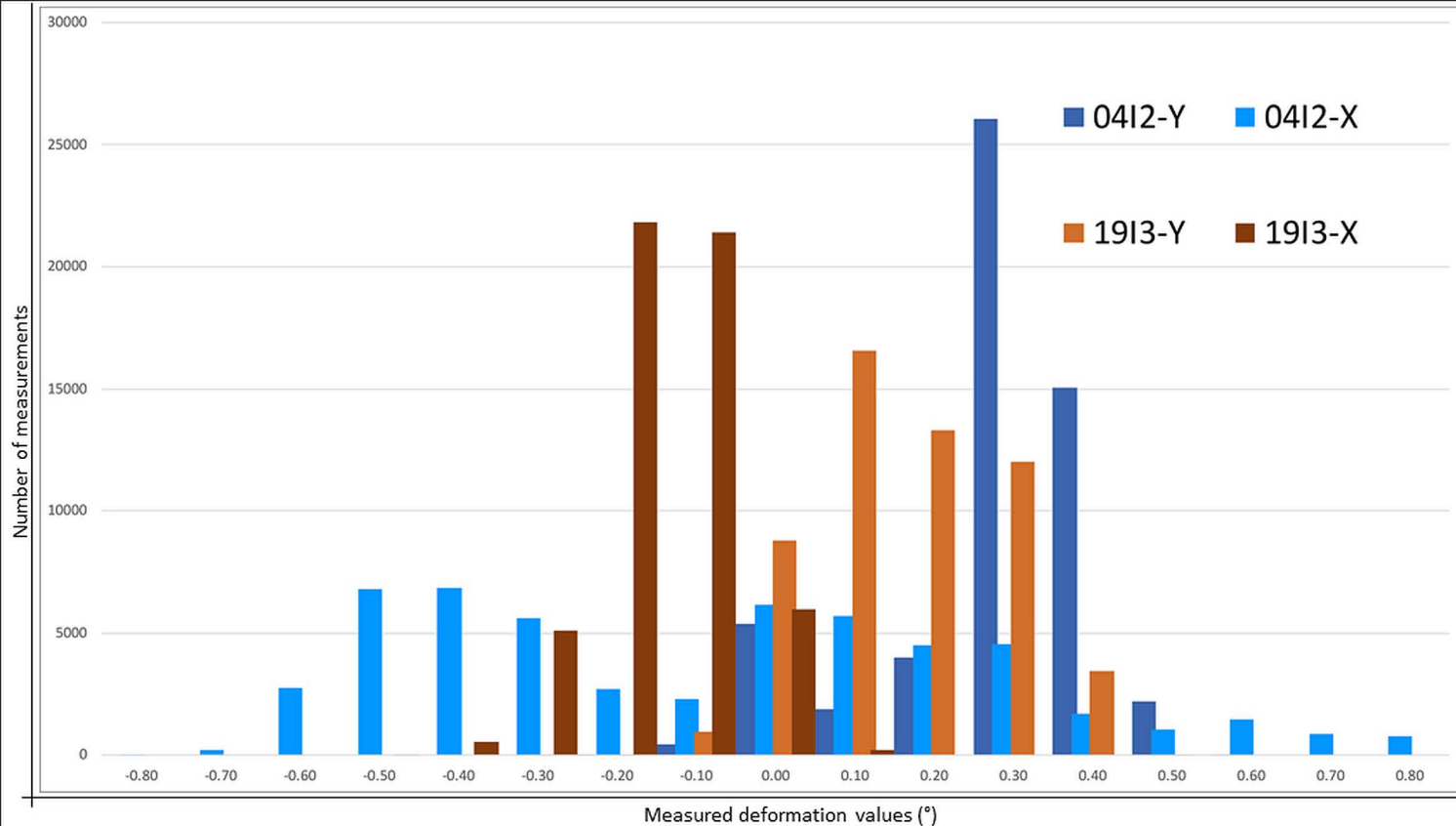


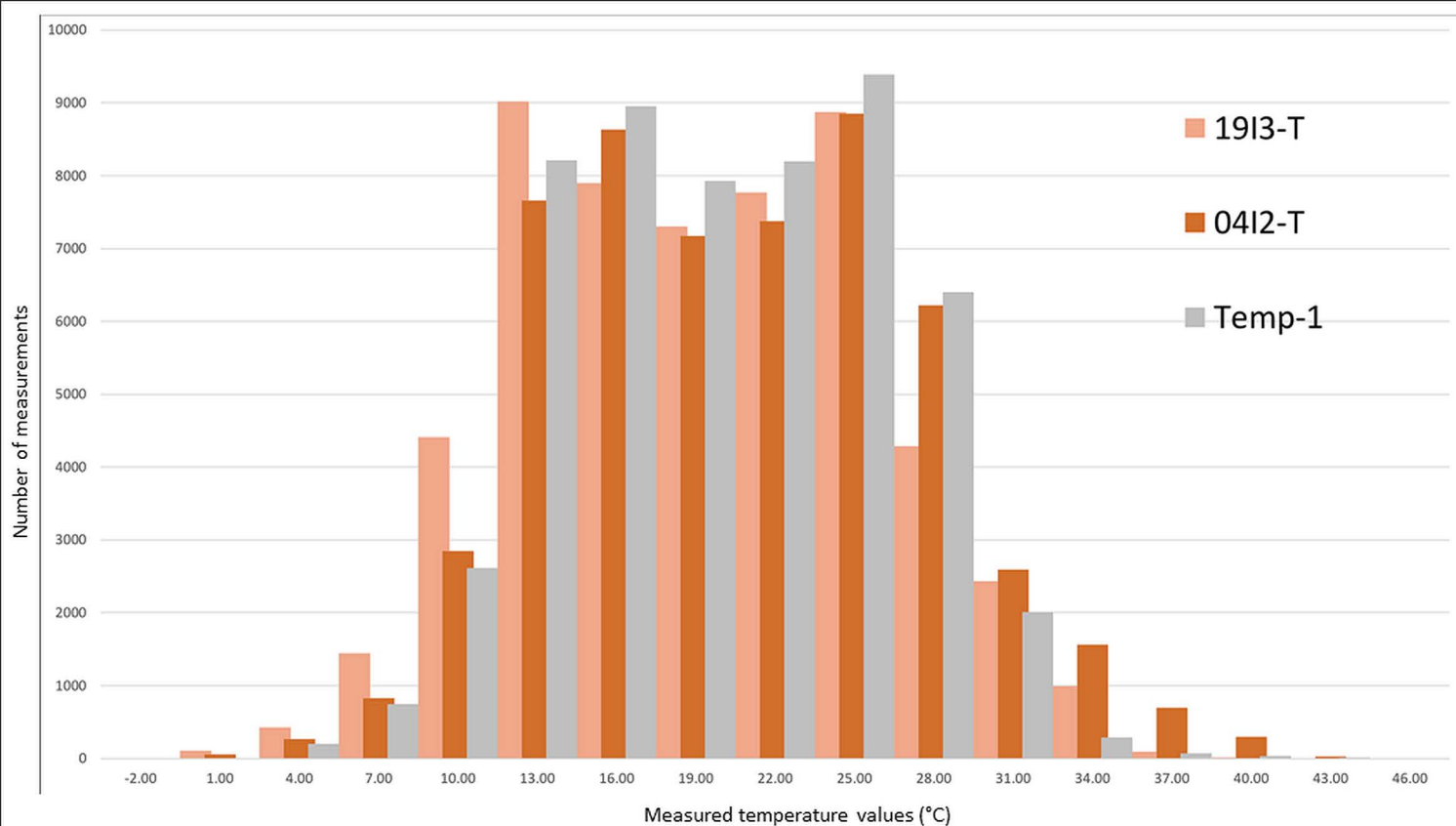


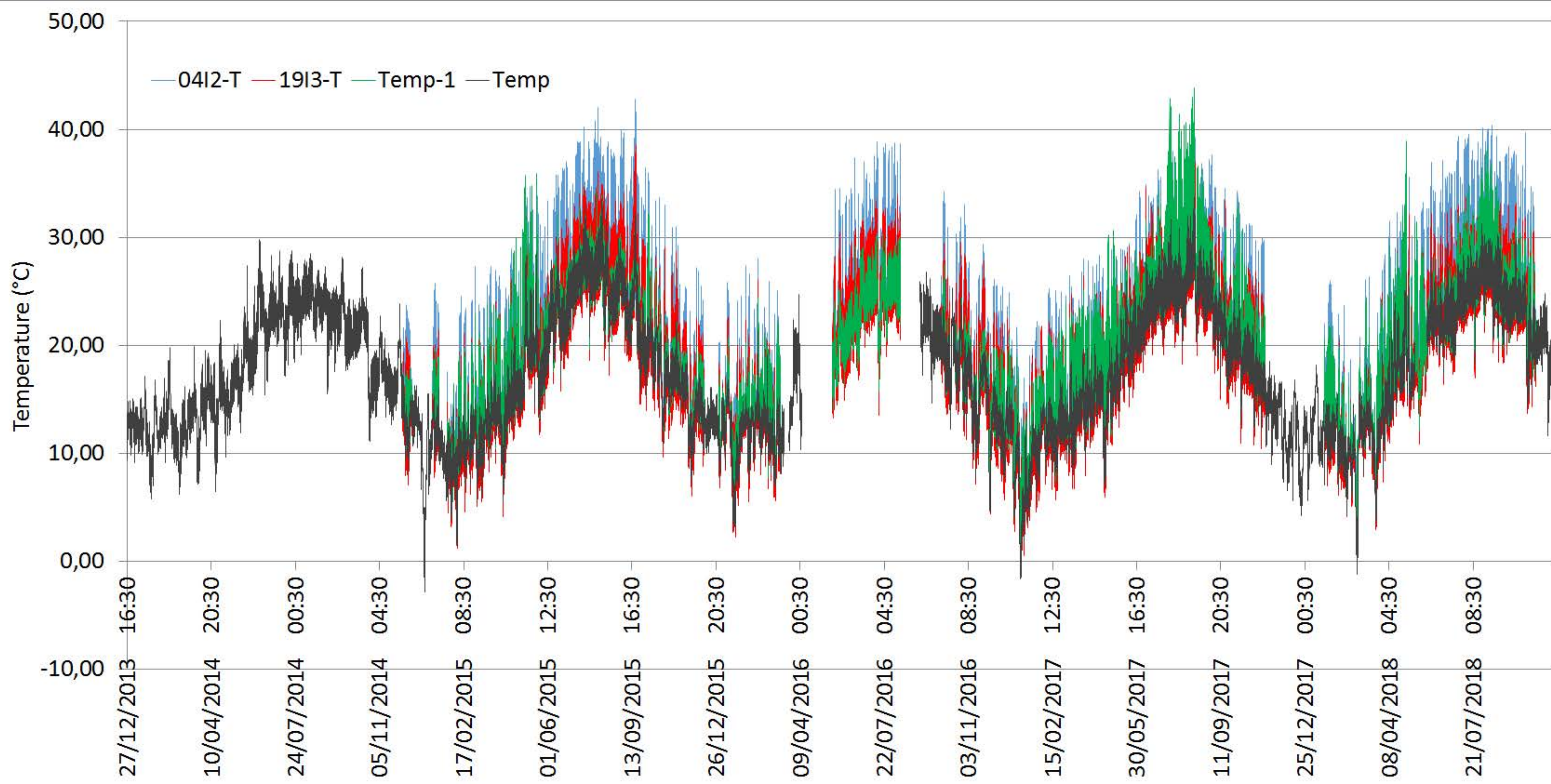


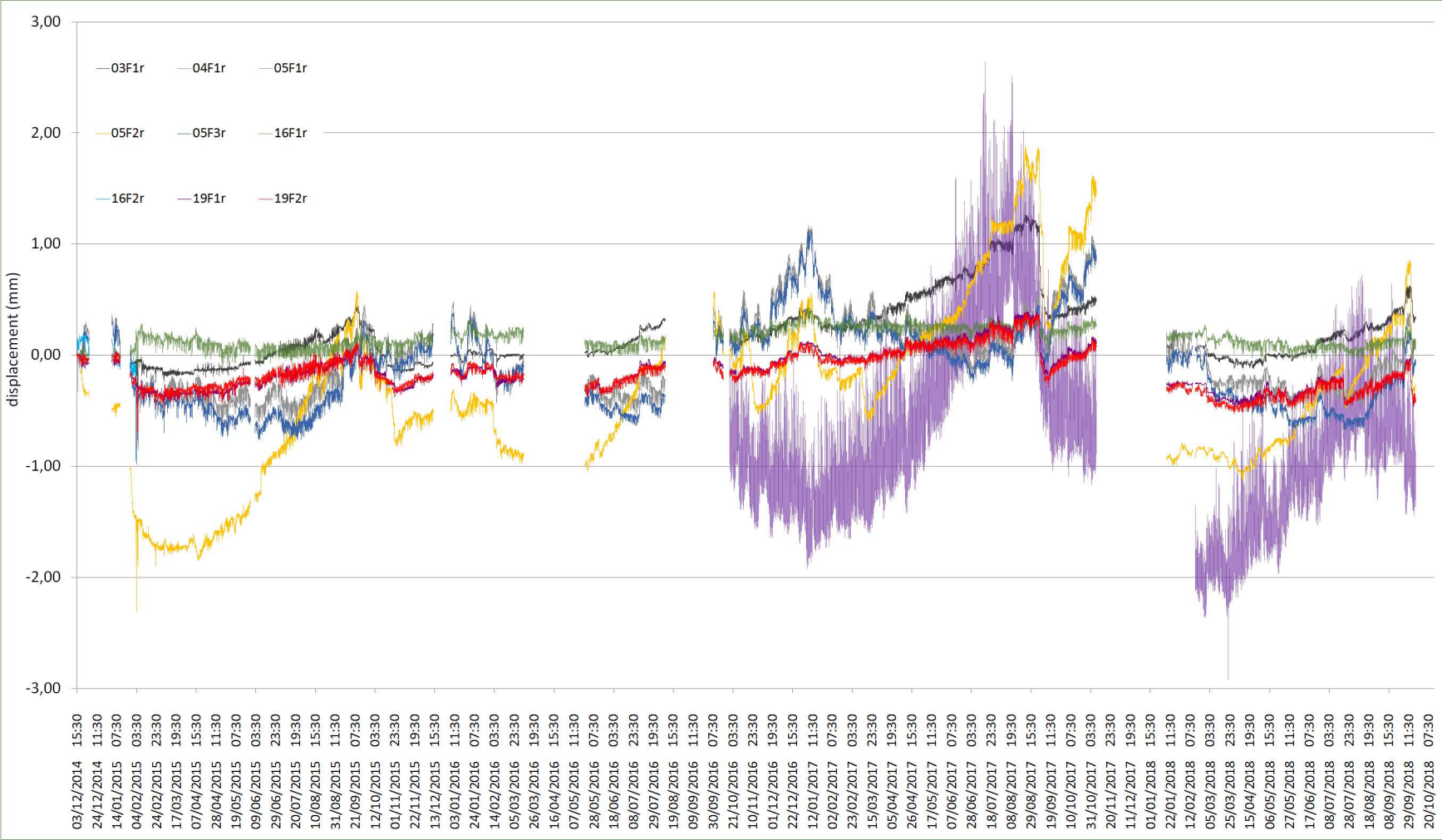


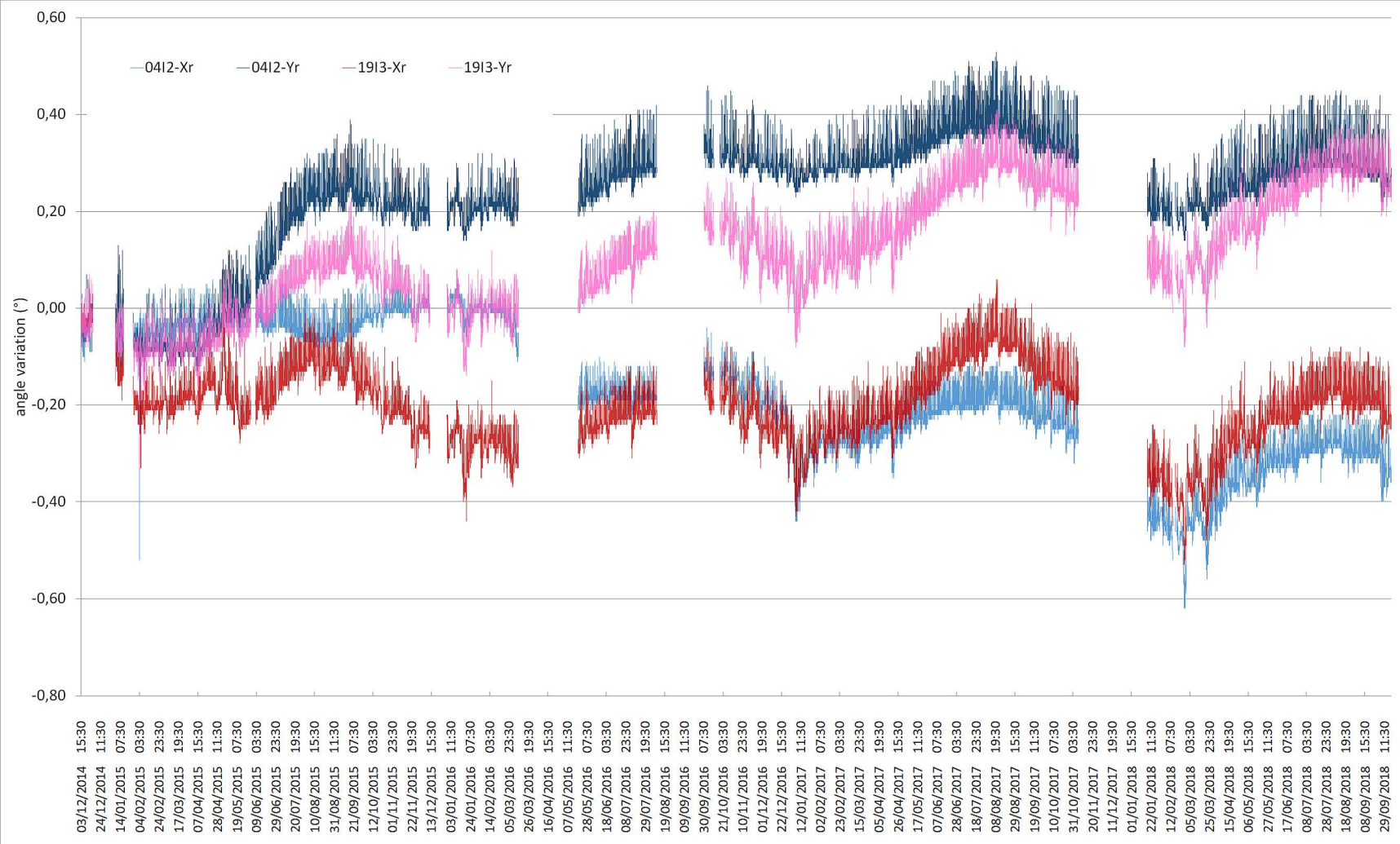


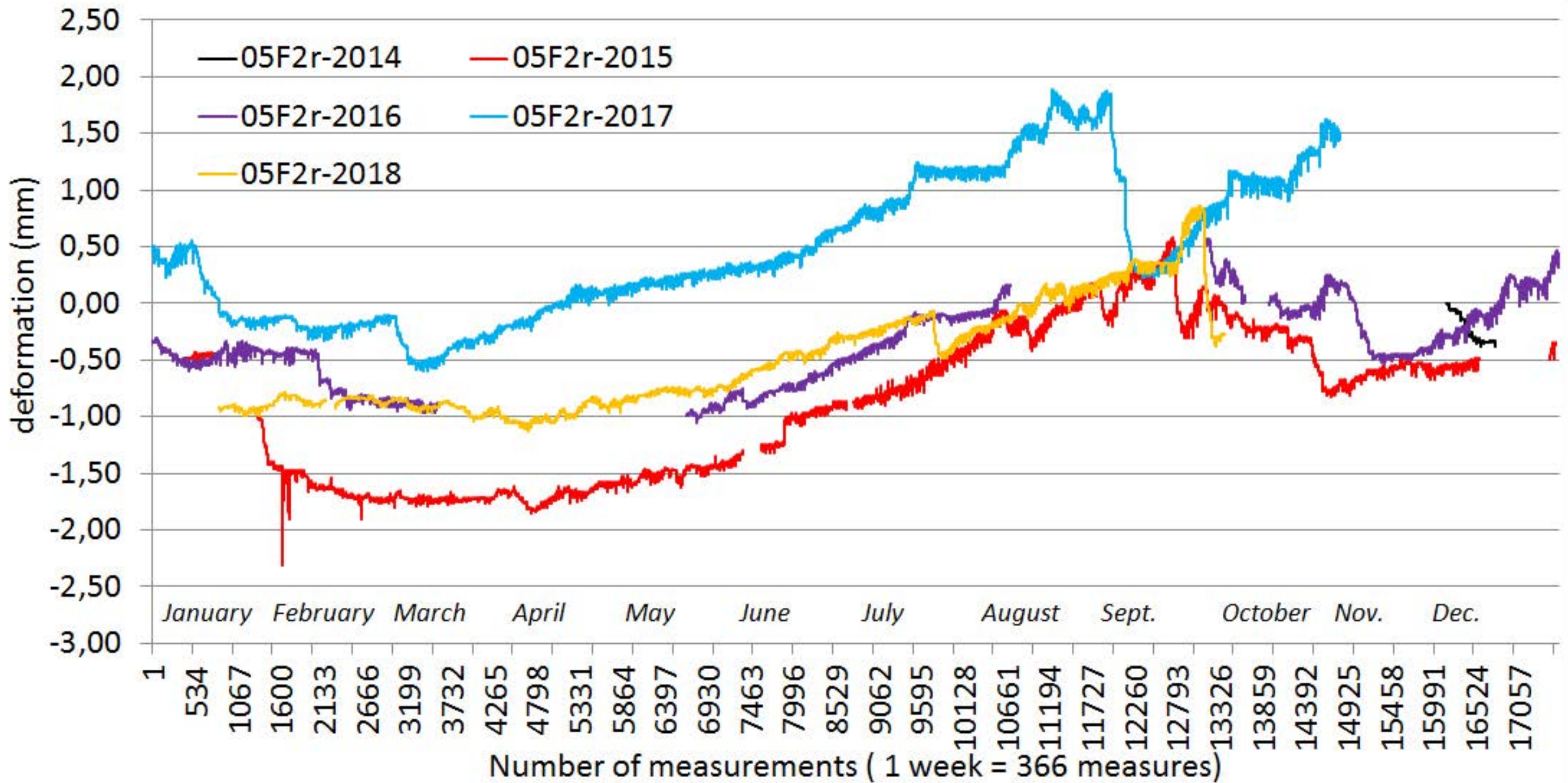












$$y = 1,462E-08x^4 - 1,259E-05x^3 + 3,135E-03x^2 - 1,860E-01x + 1,118E+01$$

$$y = 1,517E-08x^4 - 1,296E-05x^3 + 3,167E-03x^2 - 1,748E-01x + 1,503E+01$$

Tmin Tmax ΔT day – – Poli. (Tmin) - - - Poli. (Tmax)

